One-Dimensional Flame Propagation Mechanisms

J. Chris Krok
Explosion Dynamics Laboratory
Department of Aeronautical Engineering
Rensselaer Polytechnic Institute
Troy, New York

July 10, 1991

Revised 25 June 1993 and 29 June 2012

Contents

List of Figures

List of Tables

Abstract

A computational analysis was performed of a one-dimensional flame propagating from the closed end of a tube. The flow system was found to depend on the speed of the flame. For low speed flames, only a shock wave and the flame exist; for faster flames, an expansion region must be added to bring the flow to rest at the closed end of the tube. The appearance of this expansion indicates a change in flame propagation mechanism. Temperature and pressure variations with flame speed were found to be continuous through this transition, indicating that the assumed mechanisms should be correct.

Perfect gas assumptions were used throughout the analysis. A test case was run to generate P-v and x-t diagrams of the system for various speeds, as well as the aforementioned temperature and pressure plots. The test case used $R = 287$ J/kg-K, $\gamma = 1.25$, and $q = 2.307$ MJ/kg. For these values, the change in propagation mechanism was found to occur at $V_f/c_1 \approx 2.5$.

1 Introduction

This report covers the computational simulation and analysis of a one-dimensional flame propagating in a tube with one closed end. This work is very relevant to the problem of flame acceleration and, more importantly, DDT. The problem was treated in a quasi-steady manner; for each set of calculations, the flame was assumed to be traveling at a constant speed. This speed was varied from zero to the Chapman-Jouget detonation velocity. For low speeds, the flame propagation mechanism consists of only a shock wave and flame. At the highest speed, however, the ZND model of a detonation applies. This model consists of a coupled shock and flame, followed by an expansion region. It seemed likely that this expansion region would begin to appear at some intermediate speed; this was found to be true in the analysis, which is described below.

In these calculations, reactants and products were assumed to be perfect and to have identical properties. Plots were made of various temperatures and pressures versus flame speed, and P-v and x-t diagrams were generated for four specific phases of a test case. The test case used $q = 2.307$ MJ/kg, $\gamma = 1.25$, and $R = 287$ J/kg-K.

2 Analysis

The setup is shown in figure 1, with the regions of interest numbered as they are used in the analysis. State 1 is therefore the initial state of the gas. State 2 represents the shocked reactants, while state 3 refers to the combustion products immediately after they come out of the flame. State 4 is the final state of the gas, after it has expanded to zero velocity. For low flame speeds, state 3 is equivalent to state 4 (see below). The left end of the tube is closed, while the right end remains open. The tube is filled with a reactive mixture and ignited at the left end. The flame propagates to the right, with the burned gas to its left. Initially, the gas in the tube is at ambient pressure and temperature P_1, T_1,

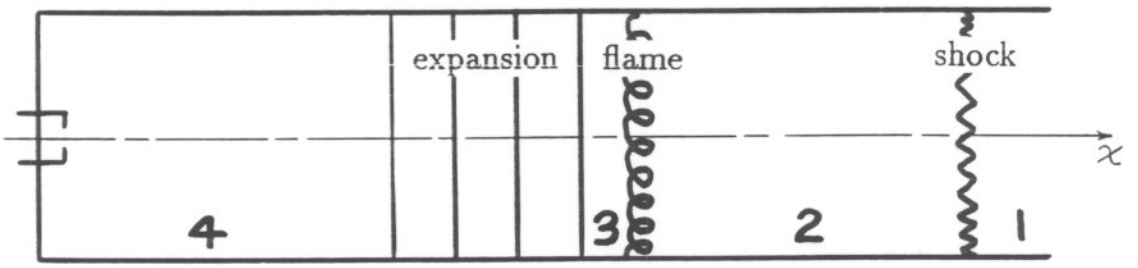

Figure 1: Basic setup of problem, showing regions used in the analysis.

and at zero velocity. Since the flame expands the gas that it burns, the gas ahead of it must move out of the tube to make room for this expansion. This is done through a shock wave that travels ahead of the flame. The shock wave imparts a velocity to the gas as it passes through, allowing the gas to move out of the tube. The faster the flame, of course, the stronger and faster the shock must be to move the unburned reactants out of the way.

Since the left end of the tube is closed, the burned gas there must have zero velocity. For low flame speeds, the flame itself will stop the gases that were put in motion by the shock wave. At some point, however, the flame velocity will become sonic with respect to the burned gas behind it. When this occurs, the flame no longer knows that the left end is closed, as perturbations in the burned gas can't keep up with the speed of the flame (they are restricted to sonic velocities). When the flame reaches this speed, an isentropic expansion fan must be inserted behind it to bring the gas fully to rest. The flame speeds are thus broken up into four phases: Phase 1, where the flame is slow enough to bring the gases to rest; Phase 2, where the flame still brings the gases to rest, but the exit velocity w_3 is sonic; Phase 3, where an isentropic expansion fan is in place; and Phase 4, when the flame speed equals the shock speed. This last phase represents the Chapman-Jouget detonation. The four phases as they would appear in the tube at a single moment in time are shown in figure 2.

The flame speed itself isn't actually the independent variable in these computations. The way that the relations are set up, it is much easier to specify the velocity of the shock wave. The relations will then determine the velocity of the flame. Also note that the velocity of the flame in the lab reference (V_f) is not the actual speed at which the flame processes the shocked gas. The lab frame velocity V_f is actually the superposition of the burning velocity, S_f, and the velocity of the gas behind the shock, u_2. All of these velocities can be interrelated through the continuity equation.

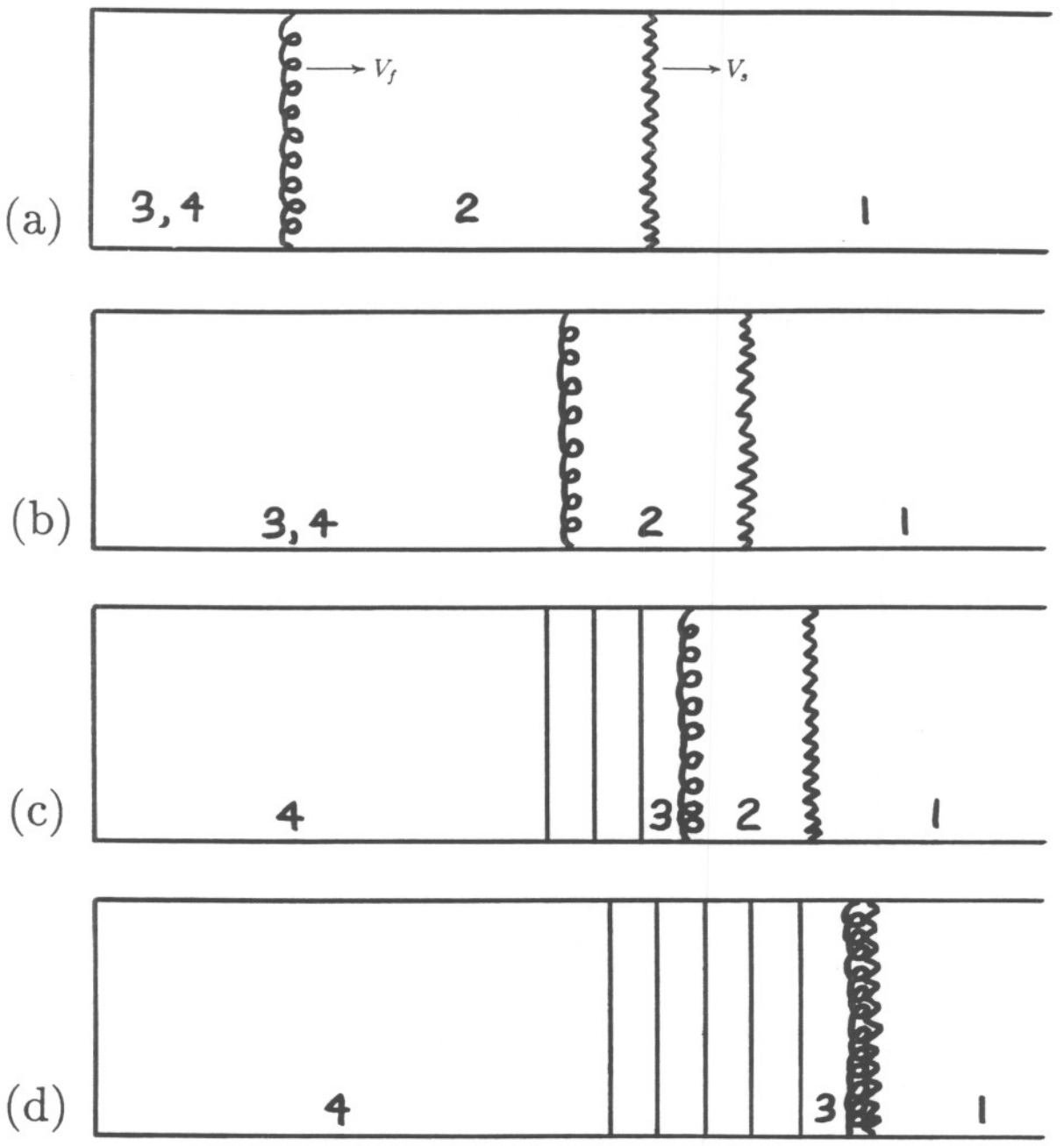

Figure 2: Situation in tube for four different phases, all frozen at same time. (a) slow flame; (b), slow flame with sonic exit; (c), flame with isentropic expansion; (d), detonation. Expansion in (c), (d) is actually continuous, although it is shown as a series of waves.

2.1 Phase 1

This phase describes the shock/flame system for a slow flame. Figure 2a shows the flame and shock in the tube, and Figure 4 shows the x-t and P-v diagrams for the system. In this phase, the speed of the flame is slow enough that it can bring the moving gas behind the shock wave to rest to satisfy the left-end boundary condition.

The equations across the shock wave are the well-known relations from gas dynamics [1, p. 72]:

$$\frac{P_2}{P_1} = \frac{2\gamma M_1^2}{\gamma+1} - \frac{\gamma-1}{\gamma+1} \tag{1}$$

and

$$\frac{v_2}{v_1} = \frac{(\gamma-1)M_1^2+2}{(\gamma+1)M_1^2}\,. \tag{2}$$

A similar relation also exists for temperature, but is much larger than these. It is much easier to use equations (1) and (2) first, and find T_2 through the ideal gas law,

$$Pv = RT\,. \tag{3}$$

Hence, by specifying the shock Mach number, M_1, all of the properties behind the shock can be found: T_2, P_2, v_2, and the gas velocity u_2 (through continuity).

Next, the change in properties across the flame are found. This is a bit more involved; we wind up creating two equations in two unknowns, P and v, but these relations are not explicit and a numerical solution to the equations must be found. This was done through the subroutine ZEROIN from Sandia National Laboratories. The equations are as follows. We start with a jump relation derived from the continuity and momentum equations [2, p. 316]:

$$[w]^2 = -[P][v]. \tag{4}$$

The brackets denote a difference in a quantity across the flame, e.g. $[P] = P_3 - P_2$, and the relative velocities are shown in figure 3.

Substituting from the quantities in figure 3, we get

$$u_2^2 = -(P_3 - P_2)(v_3 - v_2)\,. \tag{5}$$

This equation is solved for $(P_3 - P_2)$ and substituted into the Rankine-Hugoniot equation [2, p. 317],

$$h_3 - h_2 = (P_3 - P_2)\frac{(v_3+v_2)}{2} \tag{6}$$

to give

$$h_3 = h_2 - \frac{(v_3+v_2)u_2^2}{2(v_3-v_2)}\,. \tag{7}$$

Using constant properties and the ideal gas law, we can write

$$h_3 = \frac{\gamma RT_3}{\gamma-1} = \frac{\gamma P_3 v_3}{\gamma-1}\,. \tag{8}$$

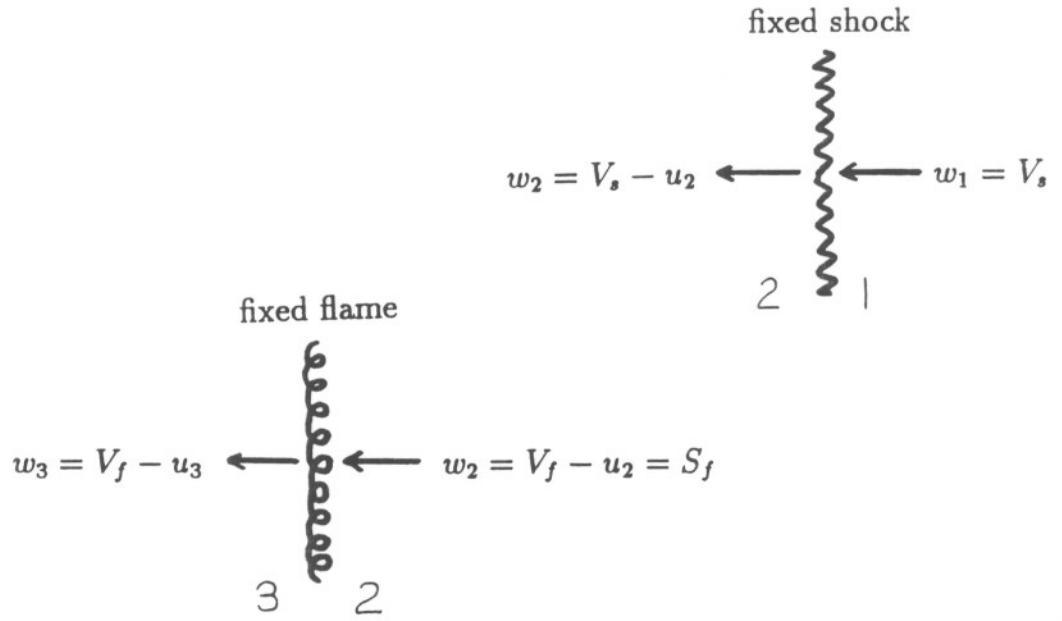

Figure 3: Shock and flame independently fixed, showing relative velocities used in equations

Putting all of this together, we get

$$P_3 = \frac{\gamma - 1}{\gamma v_3} \left[h_2 - \frac{(v_3 + v_2)u_2^2}{2(v_3 - v_2)} \right], \tag{9}$$

where

$$h_2 = \frac{\gamma P_2 v_2}{\gamma - 1} + q \tag{10}$$

and q is the heat of combustion of the fuel.

To get a second equation for P_3 in terms of v_3, the Rankine-Hugoniot equation alone can be rearranged and combined with (8) to give

$$P_3 = \frac{h_2 - \frac{1}{2}P_2(v_3 + v_2)}{v_3 \frac{\gamma}{\gamma - 1} - \frac{1}{2}(v_3 + v_2)} \tag{11}$$

where h_2 is again given by (10).

Since the shock Mach number and the initial conditions are known, P_2, v_2, and u_2 are known. So, we have two equations in two unknowns, P_3 and v_3. These are solved by the routine ZEROIN. Since ZEROIN needs an initial guess for one of the variables, $v_3 = 4v_2$ is substituted, since the flame expands the gas. ZEROIN then returns the proper values for both of the variables, which specifies the state of the gas next to the

wall. Temperature T_3 is found through the ideal gas law. The flame velocity V_f is found through the continuity equation, which reduces to:

$$V_f = \frac{u_2}{1 - v_2/v_3} \,. \tag{12}$$

Finally, as seen from the flame velocity specifications in figure 3, $S_f = V_f - u_2$.

The situation inside the tube is shown in figure 2a. The shock, traveling faster than the flame, puts the gas in the tube in motion to allow for the expansion of the gas through the flame. The flame then comes along, expanding the gas and bringing it to a rest to satisfy the left-end boundary condition ($u_4 = 0$). Note that for this phase, state 4 is equivalent to state 3, since there is no expansion fan present.

Figure 4a is the x-t diagram for this phase. Here it is easy to see that the shock is moving faster than the flame, and that the gap between them continually increases. The P-v diagram for this phase is figure 4b. In a P-v diagram, the shock adiabats show all of the possible states that can be arrived at through a shock from a given initial state. In this case, we are starting at state 1. The actual final state depends on the strength of the shock itself. Note that the end point, state 2, must lie *above* state 1 on the pressure axis. This indicates a compression shock; rarefaction shocks, where pressure decreases, are not allowed by the second law of thermodynamics. The flame is represented by the straight line from state 2 to state 3, which is known as a Rayleigh line. The slope of this line is seen to be negative, which it must be for mathematical reasons. (Basically, the slope of the Rayleigh line is equal to $-\dot{m}^2$, where $\dot{m}$ is the mass flux through the flame. Since $\dot{m}^2$ must always be positive, the slope must always be negative to match the sign of $-\dot{m}^2$.)

2.2 Phase 2

Phase 2 simply represents the upper limiting case of phase 1. The flame speed V_f is now sonic with respect to the gas behind it, so characteristics (which travel with sonic velocity) can just barely reach the flame. These characteristics inform the flame that the left end is closed and that the flow must be brought to zero velocity. If the flame moves any faster, it will no longer receive this information, and will not stop the flow. This will bring us into phase 3, where an expansion fan is required to stop the flow.

Figure 2b shows the situation in the tube, while 5a shows the x-t diagram for this phase. Note here that not only are both the shock and flame moving faster, but the flame is moving faster with regard to the shock. The flatter slopes of the shock and flame lines on the x-t diagram show the higher speeds, while the smaller angle between them shows the smaller difference in speed.

The P-v diagram for this phase is shown in figure 5b. Here we see that the line from state 1 to state 2 is steeper, indicating a stronger shock. Also note that the Rayleigh line still has a negative slope, as it must.

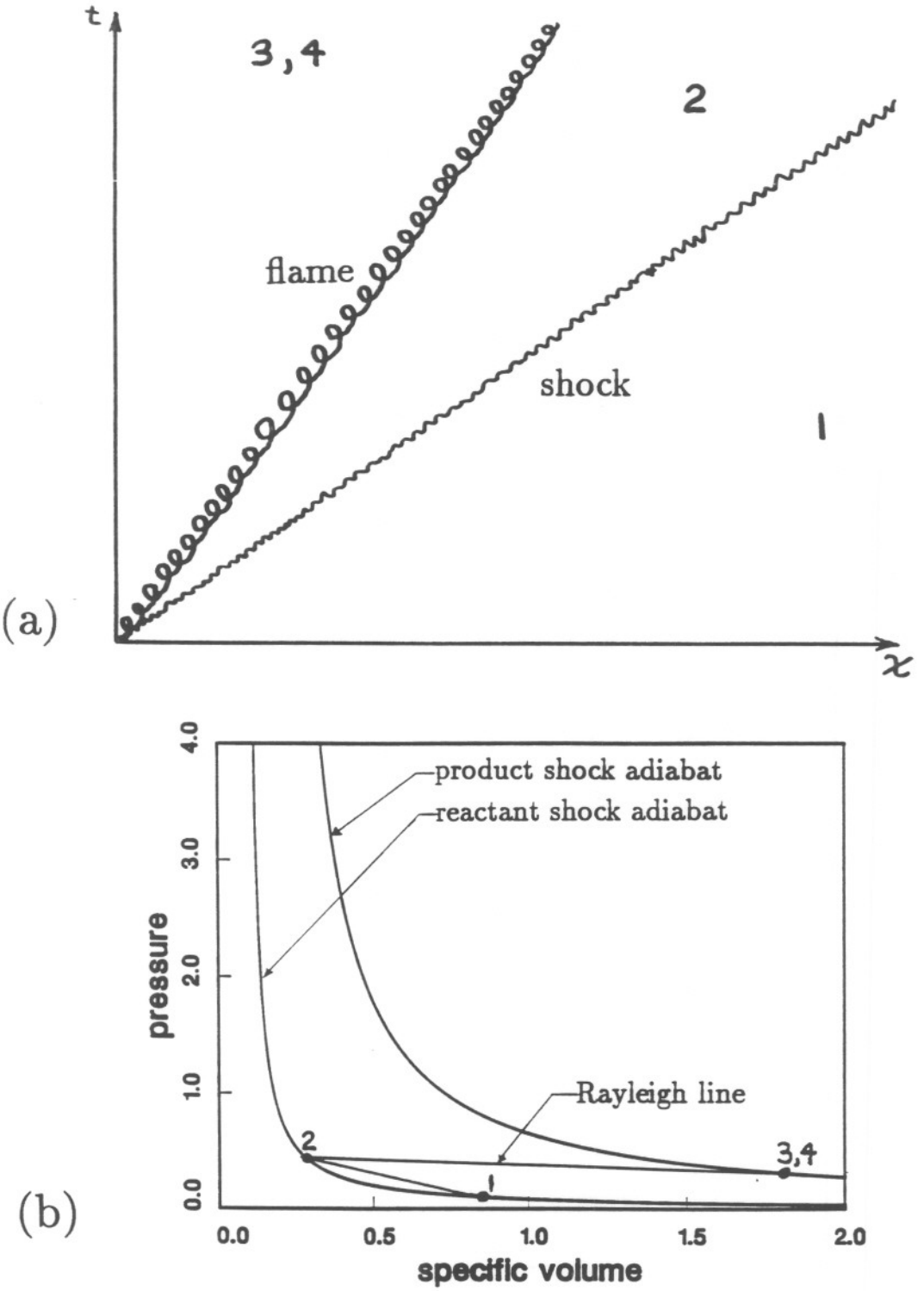

Figure 4: Phase 1 diagrams. Flame is able to bring moving fluid to rest to match left end boundary condition. (a), x-t diagram of system; (b), P-v diagram of system.

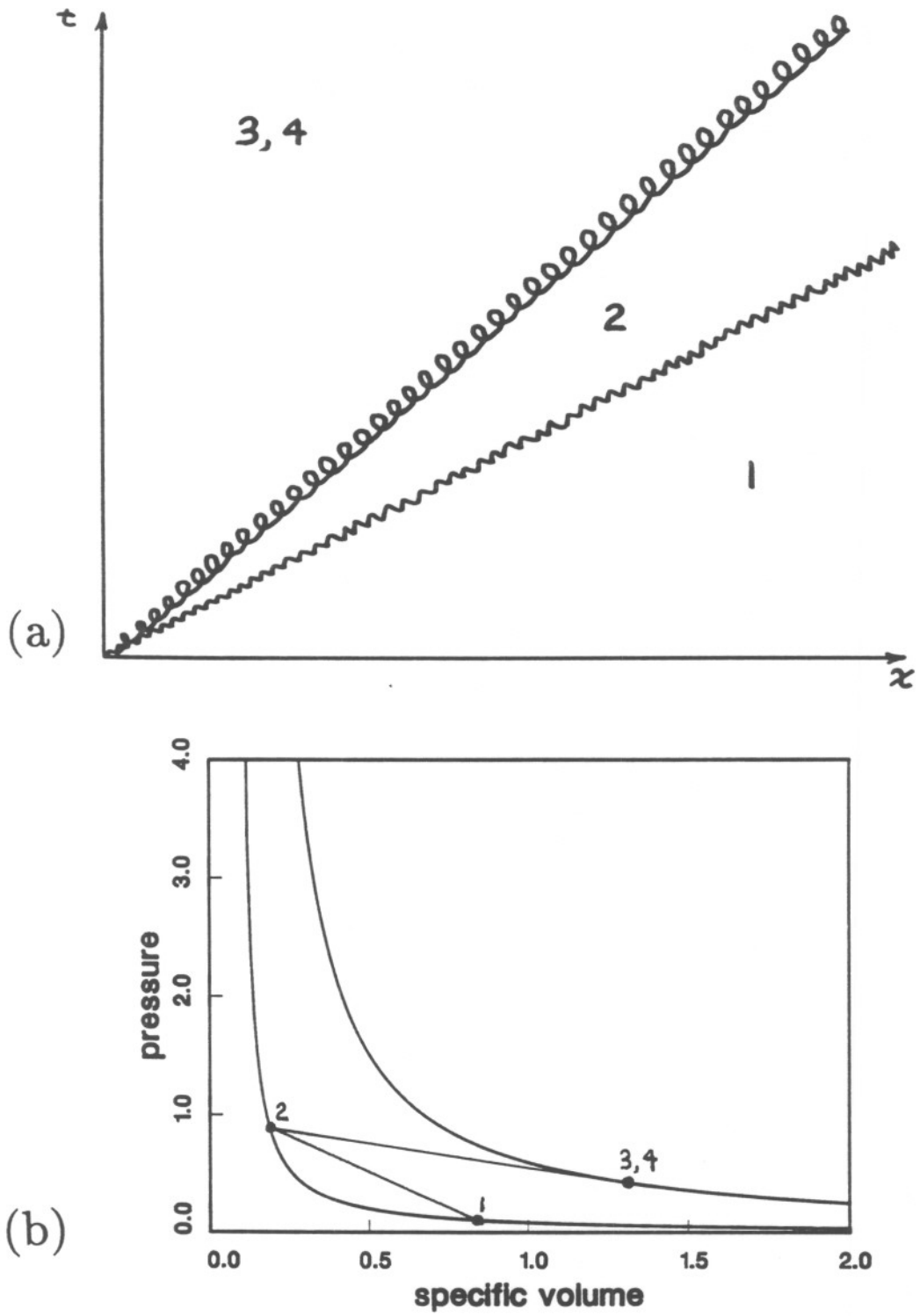

Figure 5: Phase 2 diagrams. Relative velocity of gas leaving flame (w_3) is now sonic. This is the highest flame speed for which the flame can bring moving fluid to rest. (a), x-t diagram of system; (b), P-v diagram of system.

2.3 Phase 3

In this phase, the flame is moving fast enough to require an expansion fan behind it to bring the flow to rest, but it is not up to the detonation stage yet. The major assumption of phase 3 is that the relative velocity of the flow leaving the flame (w_3,see figure 3) is sonic, or $V_f - u_3 = c_3$. Applying continuity across the flame, we get

$$V_f = \frac{v_2}{v_3} c_3 + u_2 \,. \tag{13}$$

This can be used to find an expression for $[w]$ in equation (4), and the same procedure as before is used to find an equation for P_3 in terms of v_3. Namely, we substitute the new version of (4) into the Rankine-Hugoniot equation, (6), and use (8) to generate an expression for P_3:

$$v_3 = \frac{\gamma - 1}{\gamma P_3} \left[h_2 - \frac{[c_3(1 - v_2/v_3)]^2}{2} \frac{(v_3 + v_2)}{(v_3 - v_2)} \right] . \tag{14}$$

Note that $c_3 = \sqrt{\gamma R T_3} = \sqrt{\gamma P_3 v_3}$ and that h_2 is given by (10), so the equation contains only P_3 and v_3 as variables. This time, however, P_3 is not given explicitly. Since (11) still applies, it is used first to find a value for P_3 from the guess for v_3. Then, (14) is used to find a new v_3. This all works very well with ZEROIN, and the proper values of P_3 and v_3 can be found. With these quantities specified, T_3, c_3, V_f, S_f, and u_3 can be found. (Now that the expansion fan is in place, u_3 is no longer equal to zero.)

To get the properties at the wall, the method of characteristics [2, pages 374–417] is used. Figure 6a includes a left-running (C^-) characteristic that starts at the back of the flame and runs to the wall. Since this is an isentropic expansion, the C^- characteristic has a constant value along its path, the value known as the Riemann invariant. For a perfect gas, the Riemann invariant of a C^- characteristic is given by

$$J^- = u - \frac{2}{\gamma - 1} c \,. \tag{15}$$

Immediately behind the flame, both c and u are known, so J^- can be found. At the wall, $u = 0$, so the soundspeed c_4 can be found. The soundspeed, of course, gives the temperature. P_4 can then be found through the isentropic relation

$$\frac{P_4}{P_3} = \left(\frac{T_4}{T_3} \right)^{\frac{\gamma}{\gamma - 1}} \tag{16}$$

and state 4 is fixed.

Figure 2c shows the shock, flame, and expansion fan in the tube. The expansion is shown as a series of discrete waves for clarity; in reality, this is a continuous process. The wave system is also shown on the x-t diagram for this phase, figure 6a. The shock and the flame are both moving faster than before, and the speed of the flame is approaching that of the shock.

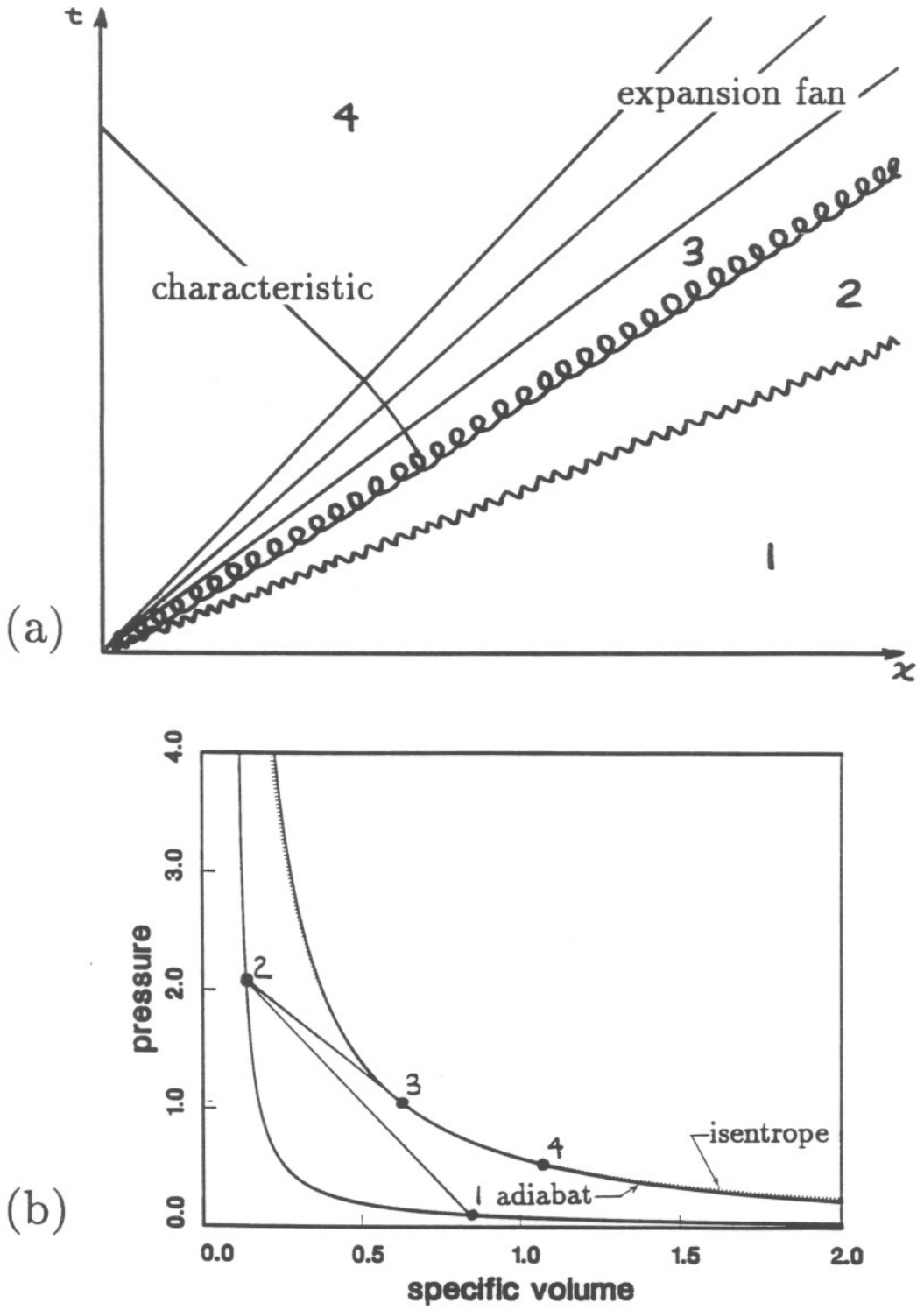

Figure 6: Phase 3 diagrams. Relative velocity of gas leaving flame (w_3) is assumed to still be sonic. Isentropic expansion must now be used to bring the fluid to rest. Note that the expansion is drawn as a series of discrete waves for convenience; this is actually a continuous process starting immediately behind the flame. (a), x-t diagram of system; (b), P-v diagram of system.

Figure 6b, the P-v diagram for phase 3, shows the effect of the expansion fan. The stronger shock gives a higher jump from state 1 to state 2 on the shock adiabat, and a steeper Rayleigh line connects states 2 and 3. The expansion between states 3 and 4 is shown on the isentrope for those states. In this diagram, the dashed line represents the isentrope, and we see that it is almost directly superimposed on the adiabat for state 3. This is expected, as an adiabat can be approximated by an isentrope for small changes in pressure.

2.4 Phase 4

This phase represents the maximum steady speed attainable by the system, the Chapman-Jouget detonation velocity (U_{CJ}). This phase is the upper limit of phase 3, and is solved through the same equations. At this point, the flame speed V_f and the shock speed are the same. Both proceed forward in a coupled fashion.

Figure 2d shows the detonation wave in the tube, followed by the expansion fan. The x-t diagram, figure 7a, also shows the shock and flame proceeding forward as a detonation. Figure 7b, the P-v diagram, shows an interesting fact of the C-J detonation phase. The shock wave takes the reactants from state 1 to state 2 on the lower adiabat, and the line connecting these states is tangent to the adiabat of the products. State 3 lies at the point of tangency. This is the definition of the C-J detonation, and is the point at which the products exit the detonation with sonic velocity. Immediately after exiting the detonation, the products expand along the isentrope to state 4. Again note the high coincidence of the shock adiabat and the isentrope in the region of interest.

3 Results

The results for the specific case that was simulated are shown in tables 1-3, and the same data is plotted in figures 8 through 13. As stated previously, the calculations are done by specifying the Mach number of the initial shock, M_1. Then, using the equations outlined in the analysis, all of the states and the flame speed can be found. The Mach numbers used run from zero, which is the constant-pressure combustion case, up to the C-J Mach number, which was found to be approximately 5.2 for the test case.

As the Mach number is increased from zero, the flame speed is checked against the soundspeed in region 3-4 at every increment. Since the gas in region 3-4 is at rest, the flame speed V_f is equal to the relative speed at which the gas leaves the flame. When $V_f = c_3$, the system is at phase 2. All of the lower Mach numbers fall in the phase 1 regime. Once phase 2 is hit, the program switches to the next set of equations, which govern phases 3 and 4. The system is in phase 3 until the flame speed V_f matches the speed of the shock, at which point the system in phase 4. Note that phases 2 and 4 are single points which are special cases of phases 1 and 3, respectively. For the test case, phase 2 was found to occur at $M_1 \approx 2.8$, or $M_{f,1} \approx 2.5$, where $M_{f,1} = V_f/c_1$.

At this point it is interesting to note that the mathematics provided solutions beyond the phases for which they were derived and valid. Initially, when only the first set of

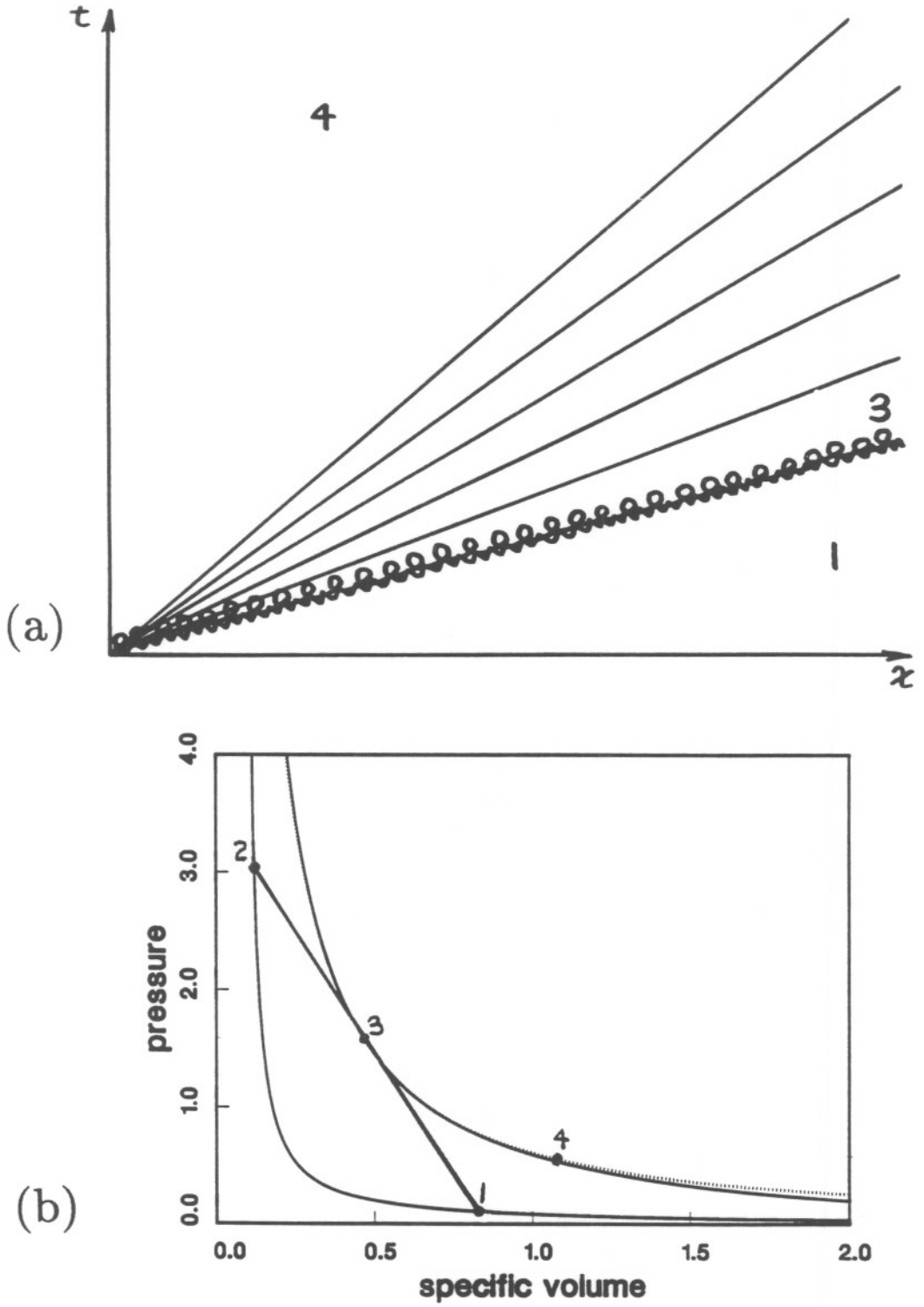

Figure 7: Phase 4 diagrams. System is now at detonation stage. Flame and shock are coupled, and travel at the same velocity, U_{CJ}. (a), x-t diagram of system; (b), P-v diagram of system.

equations was programmed, we expected some sort of singularity to occur when the Mach number M_1 passed the phase 2 point. We expected a non-solveable set of equations or some other pathology that would indicate the passing of phase 2. However, when we ran the program, it continuously provided solutions for as high a shock Mach number as we put in. Thus, we had to use the method of comparing V_f to c_3 to see when the flame could no longer detect the closed end of the tube. At that point, the program switched to the second set of equations, as mentioned above. While the equations seemed to be mathematically correct, we knew that the answers were not physically correct, so we had to watch that part independently.

Likewise, when the second set of equations was added to the program, we expected some mathematical problem to crop up when the system hit the C-J detonation phase. Again, the program went on cranking out solutions well beyond the C-J point, although it did come up with a square root of a negative number further on. Looking at the solutions, we saw that the computed V_f began to *exceed* the velocity of the shock wave! Since the flame is what produces the shock wave in the first place, this makes no sense physically, and the program was stopped when $V_f = V_s$. This point was taken to be phase 4, the C-J point.

All of the temperatures and pressures were normalized with respect to their initial values for plotting, and were plotted against the flame speed normalized to initial sound-speed (V_f/c_1). Figure 8 shows the temperature behind the shock. This is standard shock relation stuff.

Figure 9 shows the temperature immediately following the flame. This is seen to rise slightly and level off before the phase 2 point. At that point, there is a discontinuous change in slope, which is caused by the change in propagation mechanism. Fortunately, the function itself is still continuous at that point, indicating that we have the correct mechanisms on either side. More importantly, left-end temperature T_4 is totally continuous, even at the change in mechanism. This plot is shown in figure 10.

Figures 9 and 10 are both identical from $M_{f,1} = 0$ to $M_{f,1} = 2.5$, since there is no expansion fan for these Mach numbers and regions 3 and 4 are effectively the same.

The pressures are shown in figures 11–13. Figure 11 shows the pressure after the shock wave; once again, this is standard shock stuff. Figure 12 shows the pressure immediately behind the flame, P_3. As in the temperature plot for state 3, there is a discontinuity in slope at $M_{f,1} = 2.5$. This is again due to the change in mechanism. We see that the pressure sharply increases at that point, since the flame itself no longer has to expand the flow to zero velocity. Figure 13 shows the pressure after the expansion fan, P_4. This plot, as the plot for T_4, appears to be fully continuous, showing that we have used the correct mechanism in all phases. Finally, figures 12 and 13 are identical up to $M_{f,1} = 2.5$, since there is no expansion fan there and states 3 and 4 are effectively the same.

4 Conclusion

This report documents the computational simulation of a flame traveling at speeds ranging from zero to the C-J detonation velocity. The simulation was one-dimensional and

inviscid, and perfect gas laws and assumptions were used throughout. We found that the structure of the system changes continuously from the slow-flame phase to the detonation phase, with an expansion fan beginning to exist at some intermediate speed. For the conditions used for our example computations, the expansion fan appears when the flame Mach number (based on the undisturbed sound speed) increases above 2.5. This appearance of an expansion fan was expected, since the ZND model for a detonation includes an expansion fan after the detonation, and the slow flame model has no expansion.

Our results are very relevant to the problem of flame acceleration and particularly the phenomena of DDT, in which the flame speeds become large enough to produce the fluid motion that causes the expansion fan. Existing models of flame acceleration are extrapolations of the simple low–speed model in which the velocity behind the flame is zero. Our present results indicate that these models will certainly fail when the flame speed reaches the magnitude associated with DDT.

References

[1] John, James E. A., *Gas Dynamics.* Allyn and Bacon, Massachusetts, 1969.

[2] Thompson, Philip A., *Compressible-Fluid Dynamics*, Philip A. Thompson, 1988.

Note: This problem was worked out a long time ago by Zel'dovich and Shchelkin (1940) and later by Gandel'man. The theory is presented in Zel'dovich and Kompaneets, Theory of Detonation, 1960, pp. 109-120. An independent derivation is given by G. I. Taylor in his article "Gas Dynamics of Combustion and Detonation" in Fundamentals of Gas Dynamics, High-Speed Aerodynamics and Jet Propulsion, Vol. III, 1958, pp. 645-653. JES 24 June 1993.

Table 1: Flame speed, V_f, and burning velocity, S_f, for the full range of shock Mach numbers.

M_s	V_f/c_1	S_f/c_1
1.0	0.0000	0.0000
1.1	0.2025	0.0328
1.2	0.3902	0.0643
1.3	0.5657	0.0939
1.4	0.7311	0.1216
1.5	0.8879	0.1472
1.6	1.0376	0.1709
1.7	1.1812	0.1929
1.8	1.3196	0.2134
1.9	1.4535	0.2325
2.0	1.5837	0.2504
2.1	1.7106	0.2672
2.2	1.8347	0.2832
2.3	1.9563	0.2983
2.4	2.0758	0.3128
2.5	2.1934	0.3268
2.6	2.3094	0.3402
2.7	2.4240	0.3532
2.8	2.5373	0.3659
2.9	2.6497	0.3785
3.0	2.7618	0.3914
3.1	2.8736	0.4048
3.2	2.9851	0.4184
3.3	3.0964	0.4325
3.4	3.2076	0.4468
3.5	3.3187	0.4616
3.6	3.4297	0.4766
3.7	3.5407	0.4920
3.8	3.6516	0.5077
3.9	3.7625	0.5238
4.0	3.8735	0.5402
4.1	3.9845	0.5569
4.2	4.0956	0.5739
4.3	4.2067	0.5912
4.4	4.3179	0.6088
4.5	4.4292	0.6267
4.6	4.5406	0.6449
4.7	4.6521	0.6634
4.8	4.7637	0.6822
4.9	4.8754	0.7013
5.0	4.9872	0.7206
5.1	5.0992	0.7402
5.2	5.2113	0.7600

Table 2: Temperatures T_2, T_3, and T_4 for the full range of shock Mach numbers.

M_1	T_2/T_1	T_3/T_1	T_4/T_1
1.0	1.0000	6.3589	6.3589
1.1	1.0431	6.3970	6.3970
1.2	1.0845	6.4249	6.4249
1.3	1.1255	6.4455	6.4455
1.4	1.1669	6.4608	6.4608
1.5	1.2092	6.4722	6.4722
1.6	1.2528	6.4807	6.4807
1.7	1.2979	6.4871	6.4871
1.8	1.3448	6.4917	6.4917
1.9	1.3936	6.4952	6.4952
2.0	1.4444	6.4977	6.4977
2.1	1.4974	6.4994	6.4994
2.2	1.5524	6.5006	6.5006
2.3	1.6097	6.5013	6.5013
2.4	1.6693	6.5018	6.5018
2.5	1.7311	6.5019	6.5019
2.6	1.7953	6.5019	6.5019
2.7	1.8618	6.5018	6.5018
2.8	1.9306	6.5015	6.5015
2.9	2.0018	6.5588	6.5021
3.0	2.0754	6.6253	6.5050
3.1	2.1515	6.6941	6.5102
3.2	2.2299	6.7650	6.5175
3.3	2.3107	6.8382	6.5271
3.4	2.3939	6.9136	6.5387
3.5	2.4796	6.9912	6.5524
3.6	2.5677	7.0711	6.5681
3.7	2.6582	7.1532	6.5858
3.8	2.7512	7.2376	6.6055
3.9	2.8466	7.3242	6.6271
4.0	2.9444	7.4132	6.6505
4.1	3.0447	7.5043	6.6759
4.2	3.1475	7.5978	6.7030
4.3	3.2527	7.6936	6.7320
4.4	3.3603	7.7916	6.7627
4.5	3.4704	7.8919	6.7952
4.6	3.5830	7.9945	6.8295
4.7	3.6980	8.0995	6.8654
4.8	3.8155	8.2067	6.9030
4.9	3.9354	8.3162	6.9423
5.0	4.0578	8.4281	6.9833
5.1	4.1826	8.5422	7.0259
5.2	4.3099	8.6587	7.0701

Table 3: Pressures P_2, P_3, and P_4 for the full range of shock Mach numbers.

M_1	P_2/P_1	P_3/P_1	P_4/P_1
1.0	1.0000	1.0000	1.0000
1.1	1.2333	1.2251	1.2251
1.2	1.4889	1.4529	1.4529
1.3	1.7667	1.6797	1.6797
1.4	2.0667	1.9026	1.9026
1.5	2.3889	2.1196	2.1196
1.6	2.7333	2.3293	2.3293
1.7	3.1000	2.5308	2.5308
1.8	3.4889	2.7234	2.7234
1.9	3.9000	2.9070	2.9070
2.0	4.3333	3.0815	3.0815
2.1	4.7889	3.2470	3.2470
2.2	5.2667	3.4036	3.4036
2.3	5.7667	3.5517	3.5517
2.4	6.2889	3.6916	3.6916
2.5	6.8333	3.8236	3.8236
2.6	7.4000	3.9481	3.9481
2.7	7.9889	4.0655	4.0655
2.8	8.6000	4.1762	4.1762
2.9	9.2333	4.4708	4.2809
3.0	9.8889	4.8007	4.3803
3.1	10.5667	5.1433	4.4746
3.2	11.2667	5.4989	4.5640
3.3	11.9889	5.8675	4.6488
3.4	12.7333	6.2493	4.7290
3.5	13.5000	6.6444	4.8050
3.6	14.2889	7.0529	4.8769
3.7	15.1000	7.4751	4.9449
3.8	15.9333	7.9110	5.0093
3.9	16.7889	8.3607	5.0703
4.0	17.6667	8.8245	5.1281
4.1	18.5667	9.3024	5.1828
4.2	19.4889	9.7946	5.2347
4.3	20.4333	10.3013	5.2841
4.4	21.4000	10.8225	5.3309
4.5	22.3889	11.3584	5.3755
4.6	23.4000	11.9091	5.4180
4.7	24.4333	12.4748	5.4586
4.8	25.4889	13.0556	5.4974
4.9	26.5667	13.6517	5.5346
5.0	27.6667	14.2631	5.5704
5.1	28.7889	14.8900	5.6047
5.2	29.9333	15.5325	5.6379

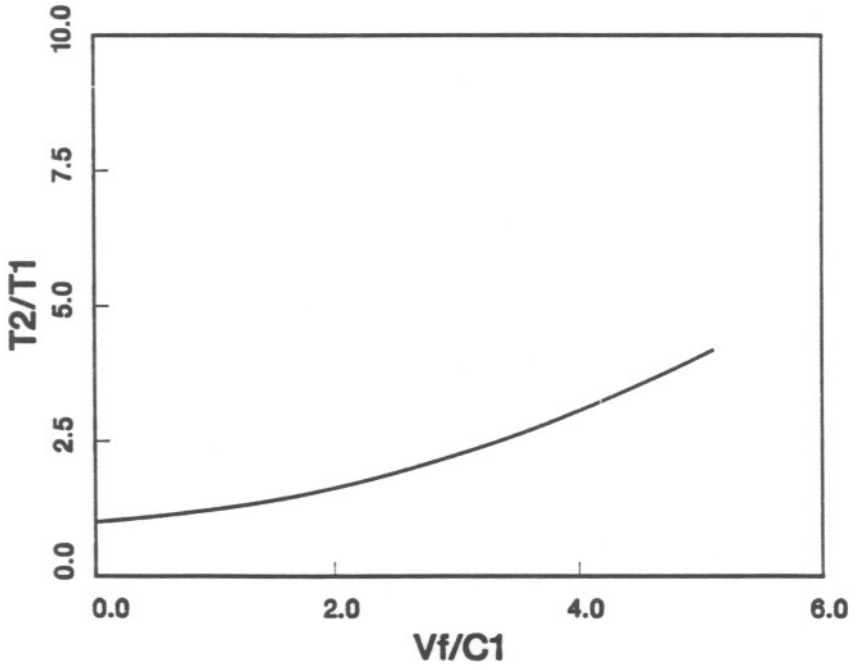

Figure 8: Post-shock temperature T_2 vs. normalized flame speed $M_{f,1}$.

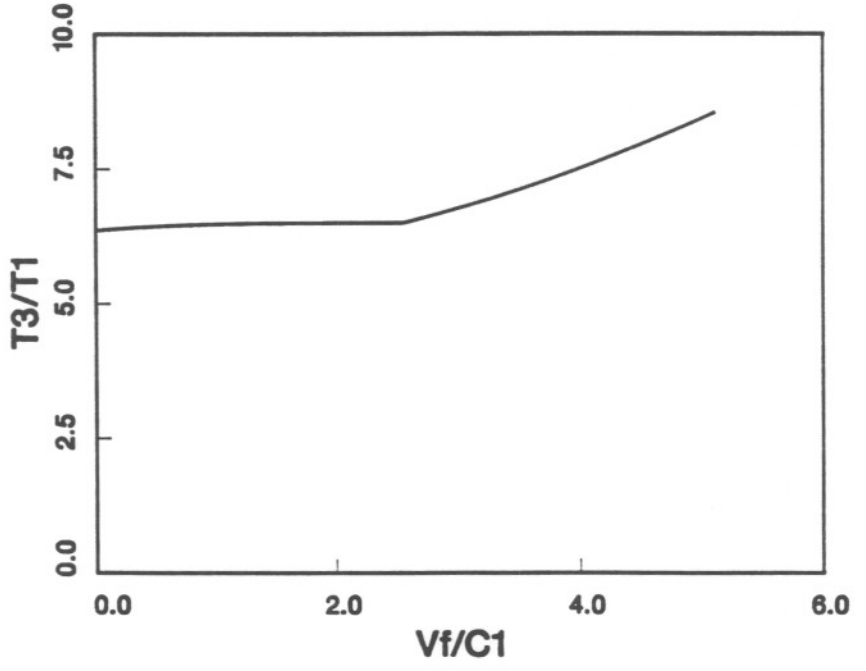

Figure 9: Post-flame temperature T_3 vs. normalized flame speed $M_{f,1}$.

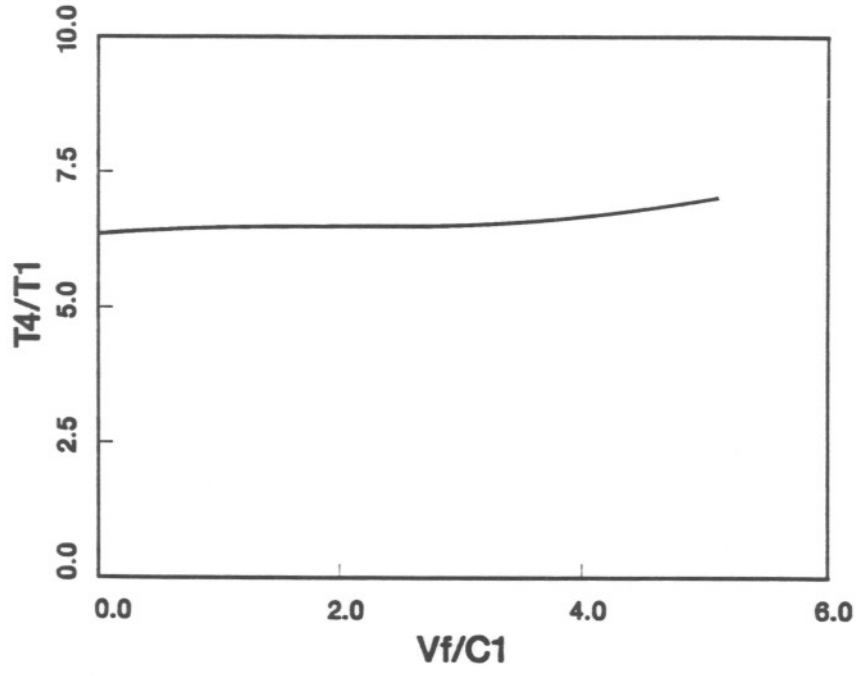

Figure 10: Post-expansion temperature T_4 vs. normalized flame speed $M_{f,1}$.

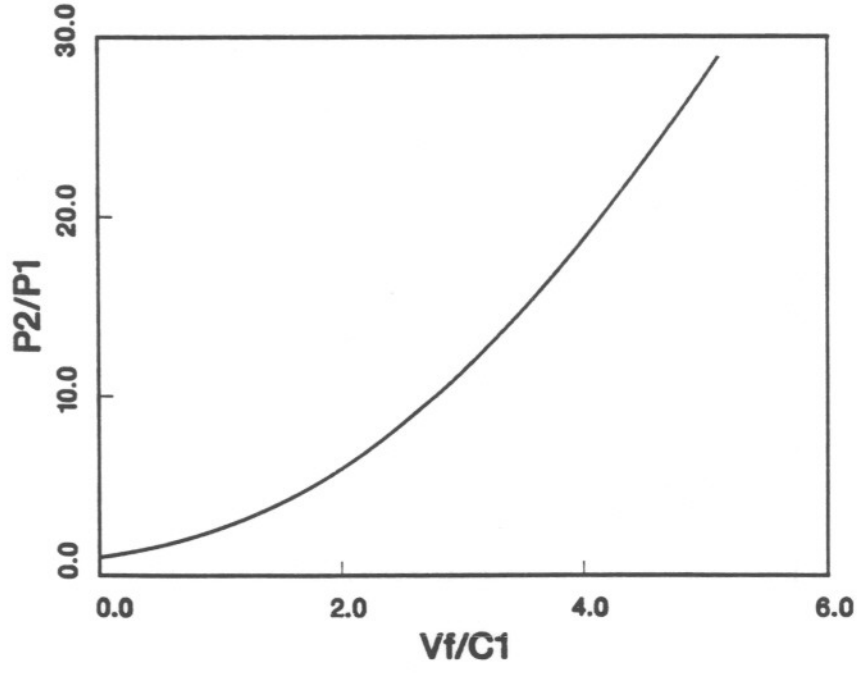

Figure 11: Post-shock pressure P_2 vs. normalized flame speed $M_{f,1}$.

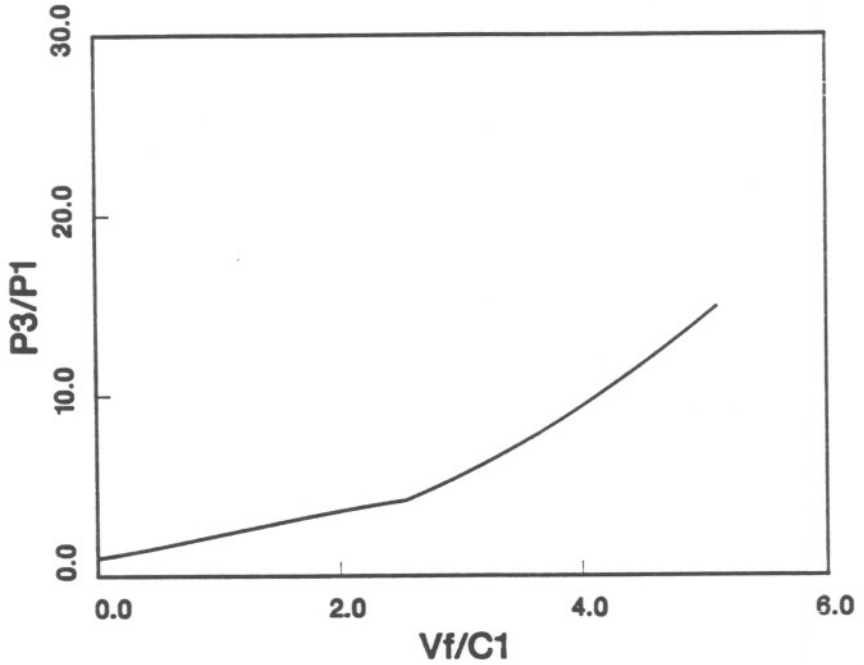

Figure 12: Post-flame pressure P_3 vs. normalized flame speed $M_{f,1}$.

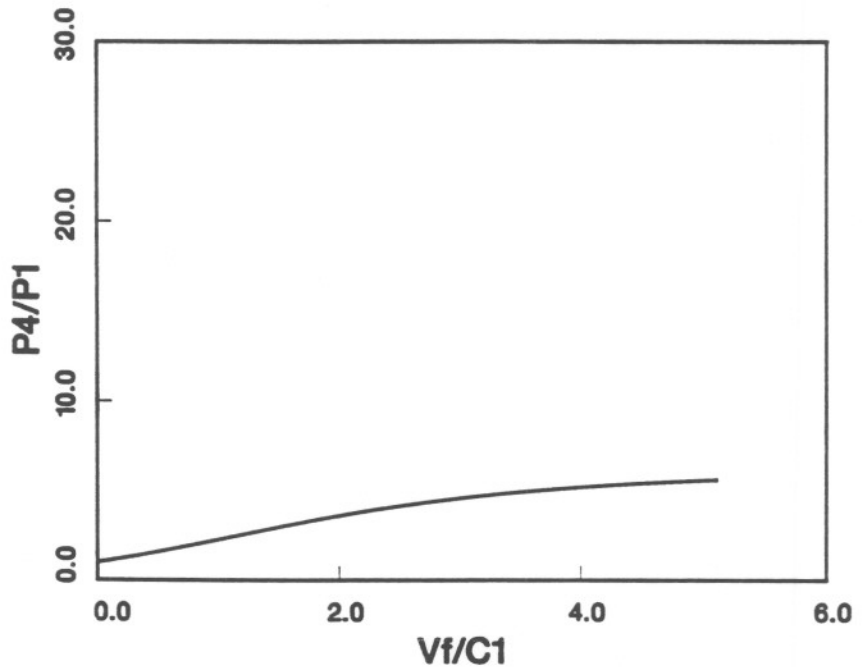

Figure 13: Post-expansion pressure P_4 vs. normalized flame speed $M_{f,1}$.

25 June 1993

Alcc pressure for this system

$$e = \frac{PV}{\gamma - 1} - \gamma q$$

$$e_0 = \frac{P_0 V}{\gamma - 1}$$

$$e_1 = \frac{P_{Alcc} V}{\gamma - 1} - q$$

$$P_{Alcc} = P_0 + (\gamma - 1)\frac{q}{V}$$

$$\frac{P_{Alcc}}{P_0} = 1 + (\gamma - 1)\frac{q}{P_0 V}$$

$$\frac{P_{Alcc}}{P_0} = 1 + (\gamma - 1)\frac{q}{RT}$$

$\gamma = 1.25$, $q = 2.307$ MJ/kg

$R = 287$ J/kg-K $\quad T = 300$

$$\frac{P_{Alcc}}{P_0} = 7.70$$

$$\frac{P_{CJ}}{P_0} = 15.5$$

29 June '12
JES

Simplified analysis of slow flame in duct

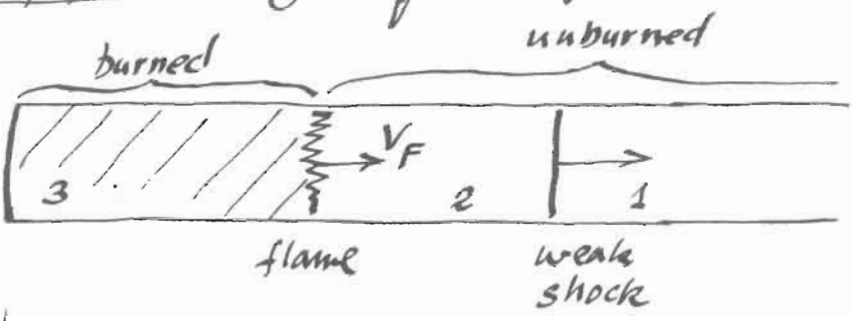

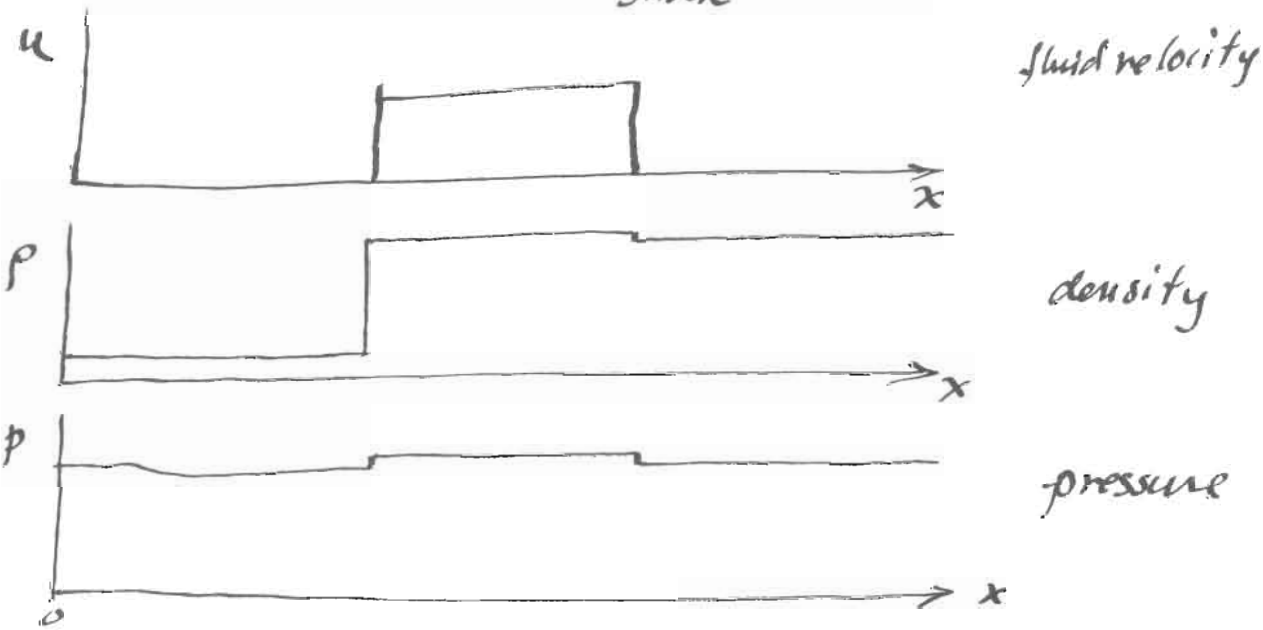

For slow flames $V_F << c_1$ = sound speed in unburned gas,

limiting case is

1) Ignore effect of weak shock on pressure (and flame) $\quad p(x,t) = p_1$

2) Ignore effect of weak shock on density and temperature.

3) velocity is $u_3 = 0$ between end ($x=0$) and flame.

$$E = \rho_u / \rho_b = \text{expansion ratio}$$

$$= \frac{R_b T_b}{R_u T_u}$$

The <u>burning speed</u> S_F is the speed of the flame relative to the flow ahead

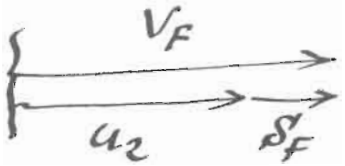

$$V_F = S_F + u_2$$

or

$$S_F = V_F - u_2$$

<u>Mass conservation</u>

Change in burned mass in time δt is

$$\delta M_b = \rho_b V_F \delta t$$

and is equal and opposite to the change in unburned gas

$$\delta M_b = -\delta M_u = \rho_u S_F \delta t$$

$$V_F = \frac{\rho_u}{\rho_b} S_F$$

$$\boxed{V_F = E S_F}$$

The induced flow velocity is

$$u_2 = (E-1) S_F$$

$$\boxed{u_2 = \left(1 - \frac{1}{E}\right) V_F}$$

If the tube is length L, the fraction of the original gas that is burned when the flame reaches the end of the tube is

$$\frac{M_b}{M_0} = \frac{\rho_b L}{\rho_u L} = \frac{1}{E}$$

An amount $M_u = M_0 - M_b = M_0\left(1 - \frac{1}{E}\right)$

is burned outside the tube

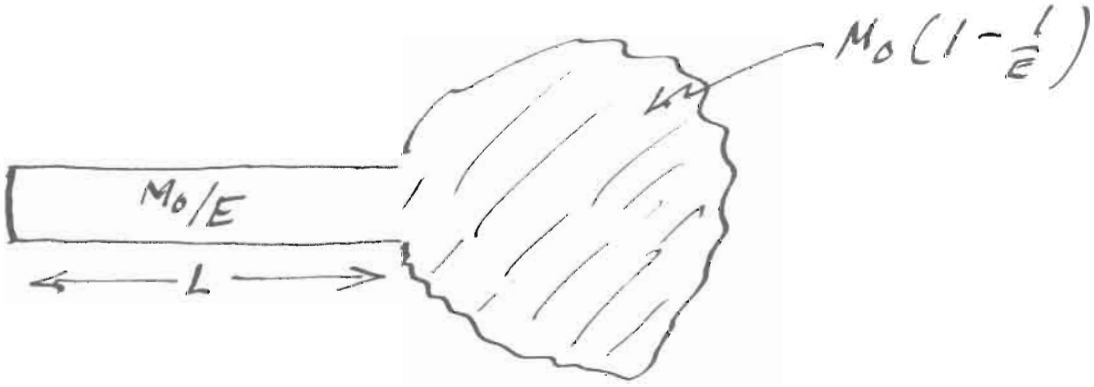

The strength of the weak shock wave ahead of flame will be

$$p' = \rho_1 c_1 u_2$$

$$= \rho_1 c_1 \left(1 - \frac{1}{E}\right) V_F$$

Example

Stoichiometric methane-air $CH_4 + 2O_2 + 7.52N_2$

9.5 % CH_4 90.5% air.

$\rho_u = 1.12$ kg/m^3 $\quad \rho_b = 0.150$ kg/m^3

$T_u = 300$ K $\quad T_b = 2225$ K

$E = 7.5$